Toward Defining the Human Parotid Gland Salivary Proteome and Peptidome: Identification and Characterization Using 2D SDS−PAGE, Ultrafiltration, HPLC, and Mass Spectrometry†

Markus Hardt,‡ Lindsay R. Thomas,‡ Scott E. Dixon,§ George Newport,‡ Nina Agabian,‡ Akraporn Prakobphol,‡ Steven C. Hall,‡,§ H. Ewa Witkowska,‡,§ and Susan J. Fisher*,‡,§,||,⊥

Department of Cell and Tissue Biology, School of Dentistry, Department of Anatomy, Department of Pharmaceutical Chemistry, and Biomolecular Resource Center Mass Spectrometry Facility, University of California at San Francisco, 513 Parnassus Avenue, San Francisco, California 94143

Received August 23, 2004; Revised Manuscript Received December 13, 2004

ABSTRACT: Saliva plays many biological roles, from lubrication and digestion to regulating bacterial and leukocyte adhesion. To understand the functions of individual components and families of molecules, it is important to identify as many salivary proteins as possible. Toward this goal, we used a proteomic approach as the first step in a global analysis of this important body fluid. We collected parotid saliva as the ductal secretion from three human donors and separated the protein components by two-dimensional SDS-polyacrylamide gel electrophoresis (2D SDS−PAGE). Proteins in gel spots were identified by peptide mass fingerprinting, and the results were confirmed by tandem mass spectrometry of selected peptides. Complementing this approach we used ultrafiltration to prepare a low-molecular-weight fraction of parotid saliva, which was analyzed directly or after reversed phase high-performance liquid chromatography separation by using mass spectrometric approaches. MS analyses of 2D SDS−PAGE spots revealed known components of saliva, including cystatins, histatins, lysozyme, and isoforms and/or fragments of α-amylase, albumin, and proline-rich proteins. We also discovered novel proteins, such as several isoforms of Zn-α-2-glycoprotein and secretory actin-binding protein. MS analyses of the ultrafiltrate showed that the low-molecular-weight fraction of parotid saliva was peptide-rich, with novel fragments of proline-rich proteins and histatins in abundance. Experiments using *Candida albicans* as the test organism showed that at least one of the novel peptides had antifungal activity. Our results show that saliva is a rich source of proteins and peptides that are potential diagnostic and therapeutic targets.

Saliva is an important determinant of oral health. Besides having a role in digestion, lubrication, and formation of a pellicle that coats and protects teeth and other oral surfaces, salivary components play a central role in regulating the oral ecology (*1*). Alterations in the composition of the oral flora and/or immune dysfunction are often linked to common oral diseases. In turn, changes in salivary composition correlate with disease susceptibility and/or progression. Hence, human saliva is a potential source of novel diagnostic markers and therapeutic targets (*2*−*7*).

In humans, the proteomes of body fluids have been studied extensively (*8*−*13*), with serum receiving the most attention (*14*). Saliva, its derivatives, and other oral fluids have also been subjected to proteomics-type analyses. Several investigators have used two-dimensional SDS−polyacrylamide gel electrophoresis (2D SDS−PAGE)[1] separation coupled with mass spectrometry (MS) to identify protein spots in samples of whole saliva (*15*−*17*), the adsorbed enamel salivary pellicle (*15*), and crevicular fluid, which bathes the gingival sulcus (*18*). On an individual basis, the proteomes of the major salivary gland secretions (parotid and sublingual/submandibular) have been mapped by 2D SDS−PAGE (*19*, *20*), but MS-based methods for protein identification have yet to be applied.

Why are proteome analyses coming to the fore? Surprisingly, DNA sequences from several different species show that the human genome, which contains ∼20000 to 25000 genes (*21*−*23*), is not sufficiently different in size to explain our functional complexity as compared with simpler organisms such as *Drosophila melanogaster*, which contains ∼13600 genes (*24*). Therefore, additional mechanisms, such as alternative splicing and posttranslational modifications (*25*, *26*), must play an important role. Salivary proteins present a rich array of posttranslational modifications: glycosylation, a particular interest of our group (*27*), and phosphorylation are important regulators of salivary protein function. Many

† This investigation was supported by a NIDCR NRSA Institutional Training Grant (T32 07204), The Sandler New Technology Fund, R37 DE07244, and U01 DE016274, P01 DE07946.

* To whom correspondence should be addressed. Tel: (415) 476-5297. Fax: (415) 502-7338. E-mail: sfisher@cgl.ucsf.edu.

‡ Department of Cell and Tissue Biology, School of Dentistry.

§ Biomolecular Resource Center Mass Spectrometry Facility.

|| Department of Anatomy.

⊥ Department of Pharmaceutical Chemistry.

[1] Abbreviations: 2D SDS−PAGE, two-dimensional SDS−polyacrylamide gel electrophoresis; MS, mass spectrometry; PRP, proline-rich protein; PMF, peptide mass fingerprint; MALDI TOF, matrix-assisted laser desorption ionization time-of-flight; MS/MS, tandem mass spectrometry; QqTOF, quadrupole/quadrupole/time-of-flight; HPLC, high-performance liquid chromatography; PRG, proline-rich glycoprotein.

10.1021/bi048176r CCC: $30.25 © 2005 American Chemical Society
Published on Web 02/01/2005

components of saliva, including acidic and basic proline-rich proteins (PRPs), statherin, histatin 1, and cystatin SA-III, have phosphorylated residues (*28*−*30*) that are required for several of the proteins' most important functions. For example, dephosphorylation of the acidic PRPs decreases binding of their phosphorylated N termini to calcium and hydroxyapatite (*31*). Loss of the latter activity is consistent with the observation that phosphorylation is required for incorporation of these proteins into the acquired enamel pellicle (*32*). Likewise, cystatin and histatin 1 binding to hydroxyapatite depends on phosphorylation (*33*, *34*), and the phosphorylated N terminus of statherin inhibits spontaneous precipitation of calcium phosphate (*35*, *36*). In contrast, the dephosphorylated form of histatin 1 retains candidacidal activity.

Increasing evidence suggests that proteolytic processing is another common posttranslational modification of salivary proteins, best illustrated by cleavages involving histatin family members. Specifically, the closely related loci *HIS1* and *HIS2* encode histatins 1 and 3 (*37*−*39*), from which all the major histatins (histatins 2 and 4 to 11) are derived by tryptic- or chymotryptic-like proteolytic processing (*40*, *41*). Histatins are highly susceptible to further proteolytic degradation, as demonstrated by the identification of smaller histatin fragments in saliva (*42*, *43*) and by the propensity of synthetic histatins to undergo processing when they are incubated with parotid saliva (*44*). Proteolytic processing has also been reported for statherins (*45*), PRPs (*46*, *47*), and cystatins (*48*). Therefore, it is not surprising that the low-molecular-weight fraction of human saliva is rich in peptides (*42*, *43*, *47*, *49*, *50*), many of which are derived from higher-molecular-weight precursors. Furthermore, many of the cleavage products have important biological functions, e.g., histatins with antifungal activities (*40*).

Here we present data that add to our knowledge of the human parotid salivary proteome. Two-dimensional SDS−PAGE coupled with MS led to the identification of additional proteins and novel forms of proteins known to be components of parotid saliva. Ultrafiltration led to the isolation of a complex fraction composed of salivary protein fragments, including the smallest fragment of histatin with candidacidal activity described to date.

EXPERIMENTAL PROCEDURES

Collection of Parotid Saliva. The protocol for collecting saliva was approved by the Committee on Human Research of the University of California at San Francisco. Informed consent was obtained from three subjects (2 male, one female, ages 30, 24, and 22, respectively) taking no medications, with no overt signs of gingivitis or caries. Parotid saliva was collected (on ice) as the subject's ductal secretion by using a Lashley cup as described previously (*51*). The saliva was clarified by centrifugation (12000*g*, 10 min) and stored at −20 °C.

Two-Dimensional SDS−PAGE. Prior to electrophoretic separation, the sample was concentrated and desalted by ultrafiltration through a Microcon centrifugal filter device (nominal molecular weight limit, 3000; Millipore Corp.). Alternatively, the saliva sample was mixed with 3 volumes of ice-cold acetone, and the protein precipitate was isolated by centrifugation (14000*g*, 10 min). The protein pellets were dissolved in rehydration buffer: 8 M urea, 2% (3-[(3-cholamidopropyl) dimethylammonio]-1-propanesulfonate), 100 mM dithiothreitol, 0.5% Pharmalyte, pH 3 to 10 or 6 to 11, and 0.002% bromophenol blue. The protein concentration was determined by using a 2D Quant kit (Amersham Biosciences). Immobiline DryStrips (13 cm, pH 3−10 L (linear) or 6−11; Amersham Biosciences) were rehydrated overnight in 250 μL of each sample that contained 100−400 μg of protein. Isoelectric focusing was performed on an IPGphor system (Amersham Biosciences) that executed a stepwise program for varying the voltage that included a desalting step. After isoelectric focusing, proteins in the IPG strips were prepared for separation in the second dimension by soaking twice for 15 min in SDS−PAGE equilibration buffer (50 mM Tris-HCl, pH 8.8, 6 M urea, 30% glycerol, 2% SDS, 0.002% bromophenol blue) supplemented with 65 mM dithiothreitol (first equilibration) and 135 mM iodoacetamide (second equilibration) (*52*). Afterward, the samples were electrophoretically separated (80 V, overnight) on precast 10−20% Tris-glycine or Tris-tricine gradient acrylamide gels (Jule Inc.) by using the Hoefer-600 electrophoresis unit (Amersham Biosciences). The gels were fixed in 45% methanol, 10% acetic acid for 1 h, and then proteins were visualized by staining for 2 h with 0.1% Coomassie R250, a modified Coomassie blue stain, dissolved in 45% methanol, 10% acetic acid. This dye and solvent combination was chosen because preliminary experiments showed that the R-type Coomassie blue stained PRPs more efficiently than the G form, a phenomenon that was previously reported (*53*−*55*). Gels were destained over 48 h in 5% methanol, 7% acetic acid. Digital images of the 2D PAGE maps were acquired using a 9800XL ScanMaker (Microtek) gel scanner. The gel images were analyzed with Phoretix 2-D Evolution software (Nonlinear Dynamics).

In-Gel Digestion. Electrophoretically separated protein spots were excised, stain-stripped three times in 50% acetonitrile/25 mM ammonium bicarbonate, pH 8.0, dehydrated with 100% acetonitrile, and dried in a Speed-Vac. Gel pieces were rehydrated with a solution of sequencing-grade trypsin (Promega), 10 μg/mL in 25 mM ammonium bicarbonate, and the digestion was carried out for 16−20 h at 37 °C. Peptides were extracted three times by the addition of 2 volumes of a solution of 50% acetonitrile/5% trifluoroacetic acid. The extracts were combined and reduced to a final volume of 5−10 μL.

Mass Spectrometry. Peptide mass fingerprinting (PMF) (*56*−*60*) was used for preliminary protein identification. Portions (typically 5%) of the unseparated tryptic digests were cocrystallized in a matrix of α-cyano-4-hydroxycinnamic acid (5 mg/mL in 50% acetonitrile/0.3% trifluoroacetic acid) and analyzed on a Voyager DE-STR MALDI TOF mass spectrometer (Applied Biosystems) operating in reflector mode. Mass spectra were produced representing protonated, monoisotopic, molecular ions $[MH]^+$ of tryptic peptides from the protein(s) present in each gel spot. The PMF spectra were externally calibrated using the Optiplate script with a peptide mixture standard (Applied Biosystems). Typical mass measurement accuracies for external calibration routines applied on a Voyager DE STR MALDI TOF mass spectrometer are ±50−75 ppm. However, in some circumstances the error can be as high as ±100 ppm. Initially, the mass accuracy tolerance for database searching was delib-

erately enlarged in an attempt to identify as many proteins as possible. After this search was completed, actual protein identifications were made if the mass measurement error precision among the experimentally observed peptides was ≤25 ppm. If poor-quality MALDI TOF mass spectra were obtained, the remainder of the sample was subjected to an additional C18 ZipTip (Millipore) cleanup step that was performed according to the manufacturer's protocol. The ZipTip eluent was spotted onto a stainless steel sample plate and analyzed by MALDI TOF MS as described above.

Preliminary protein identities were established by matching the experimentally determined peptide masses to those produced by an in silico tryptic digestion of the Swiss-Prot (http://us.expasy.org) and the NCBInr database protein sequences within the window of experimental mass measurement accuracy. The PMF searching algorithms available from MASCOT (http://matrixscience.com) (*61*) and MS-Fit (http://prospector.ucsf.edu) (*62*) were used to perform the database searches. Preliminary protein identities obtained by PMF were confirmed by acquiring tandem mass spectrometry (MS/MS) spectra of selected peptides from each in-gel digestion mixture using a QSTAR XL quadrupole/quadrupole/time-of-flight (QqTOF) mass spectrometer (Applied Biosystems) equipped with an orthogonal (o) MALDI ion source or a 4700 Applied Biosystems Proteomics Analyzer MALDI TOF/TOF mass spectrometer. Protein identification was accomplished by isolating, within the mass spectrometer, a peptide ion population with a single mass-to-charge ratio (*m*/*z*), fragmenting this population, and measuring the masses of the peptide fragment ions. The experimentally determined peptide fragment ion masses were used to search a theoretical fragment ion mass database generated by in silico digestion and fragmentation of all proteins in the Swiss-Prot and NCBInr databases using MASCOT and Protein Prospector MS-Tag algorithms. The experimental fragment ion masses were matched with theoretical peptide fragment ion masses within the window of experimental mass measurement accuracy of ±0.2 Da.

Analysis of the Low-Molecular-Weight Fraction. A 500-μL aliquot of freshly collected parotid saliva was immediately mixed with 15 μL of 0.5 M EDTA and 5 μL of a proteinase inhibitor cocktail (Sigma, Cat. No. P-2714), vortexed and clarified by centrifugation (10 min at 12000*g*) at 4 °C. As an alternative method to prevent proteolysis, the freshly collected saliva was acidified to a final concentration of 0.1% formic acid or trifluoroacetic acid before centrifugation. Then the supernatant (~450 μL) was transferred to a Microcon ultrafiltration device (molecular weight cutoff, 10000) and centrifuged (~90 min at 10000*g*) at 4 °C. The filtrate was frozen (−20 °C) until analysis. Briefly, the sample was cocrystallized with matrix (α-cyano-4-hydroxycinnamic acid or sinapinic acid) onto MALDI targets, both as a mixture and after reversed phase high-performance liquid chromatography (HPLC) separation. Liquid chromatographic separations were performed on an Ultimate Capillary HPLC System (Dionex/LC Packings) equipped with a PepMap C18 column (Dionex/ LC Packings; 300 μm i.d., 15 cm length, 100 Å pore size, 3 μm particle size), a Famos Micro autosampler, and a ProBot Micro Fraction Collector. The flow rate was 4 μL/min, and the column temperature was maintained at 40 °C. The column was equilibrated at 2% B for 20 min prior to sample injection (solvent B, 80% acetonitrile/0.08% trifluoroacetic acid; solvent A, 2% acetonitrile/0.1% trifluoroacetic acid). The binary gradient consisted of a 5-min isocratic wash at 2% B to remove salt, a linear gradient of 2% to 50% B over 45 min, followed by a column cleanup step of 95% B for 7 min. Peptide elution was monitored at 214 and 280 nm. The column effluent was mixed online using a static micromixing tee (Upchurch Scientific) with a continuous stream (2 μL/min) of α-cyano-4-hydroxycinnamic acid (7 mg/mL in 50% acetonitrile/1% ammonium phosphate) before deposition across two 100-well stainless steel MALDI sample plates (Applied Biosystems) at a frequency of one spot every 20 s. The samples were analyzed by MALDI TOF MS, MALDI TOF/TOF MS/MS and oMALDI QqTOF MS/MS. Product ion spectra were matched to sequences in the NCBInr database using MASCOT or ProteinProspector. The identities of some peptides were derived utilizing de novo MS/MS sequencing.

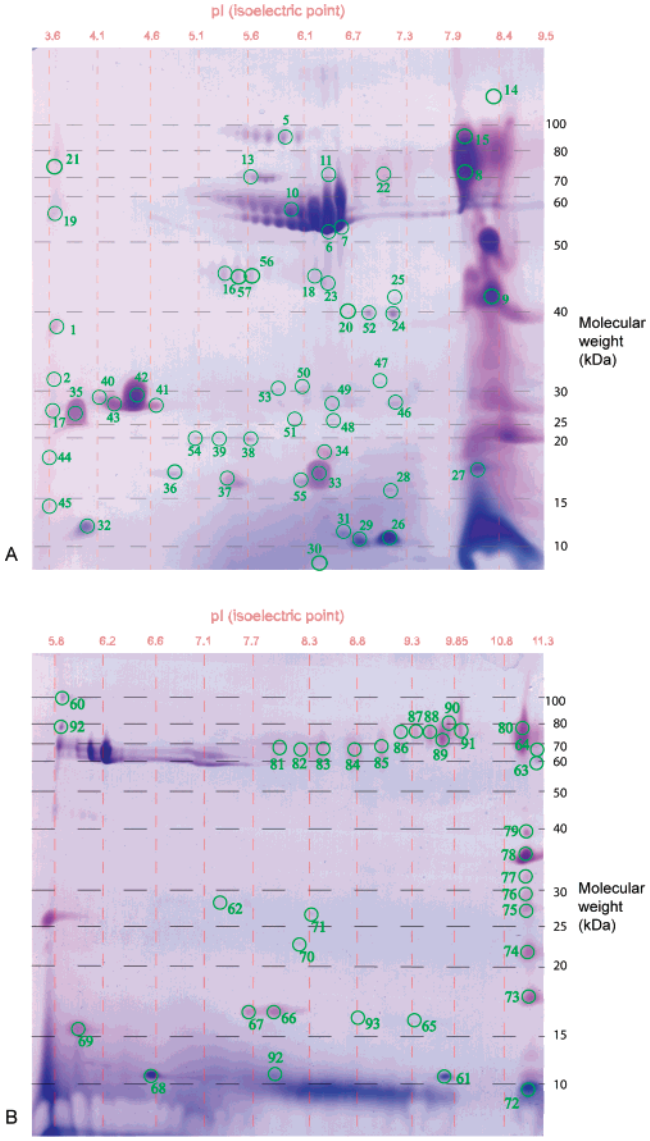

FIGURE 1: Typical 2D SDS polyacrylamide gel of human parotid saliva collected as the ductal secretion. Separation was achieved by isoelectric focusing (A, ~pH 3−10; B, ~pH 6−11) in the horizontal dimension and Tris-tricine-PAGE (10−20%) in the vertical dimension. The spots were visualized by staining with Coomassie blue R250.

Table 1: Human Parotid Proteins Detected by a Combination of MALDI TOF MS, oMALDI QqTOF MS/MS and MALDI TOF/TOF MS/MS in a Subset of the 2D SDS−PAGE Spots Labeled in Figure 1

spot ID	protein identified	Swiss-Prot/NCBI accession no.	p*I*			mass (kDa)		
			obsd	theor	Δ p*I*	obsd	theor	Δ mass
5	poly Ig receptor	P01833	5.92	5.59	−0.42	100.2	81.4	+35.9
13	serum albumin	P02768	5.61	5.67	−0.06	82.2	66.5	+15.7
16	Zn-α−2-glycoprotein	P25311	5.18	5.58	−0.40	50.4	32.1	+18.3
18	carbonic anhydrase VI	P23280	6.02	6.53	−0.50	47.6	33.6	+14.0
23	carbonic anhydrase VI	P23280	6.21	6.53	−0.32	49.5	33.6	+15.9
26	histatin 1	P15515	6.97	8.32	+1.35	11.3	4.8	+6.5
28	cystatin B	P04080	7.02	6.96	+0.06	14.6	11.1	+3.5
29	histatin 1	P15515	6.68	8.32	−1.66	11.2	4.8	+6.4
36	cystatin SA	P09228	4.75	4.85	−0.10	16.7	14.3	+2.4
41	PRP-C phosphoprotein	P02810	4.57	4.63	−0.06	23.6	15.4	+8.2
42	PRP-C phosphoprotein	P02810	4.41	4.63	−0.22	25.0	15.4	+9.6
43	PRP-C phosphoprotein	P02810	4.23	4.63	−0.40	23.8	15.4	+8.4
46	Ig κ chain C isoform	P01834	7.15	5.58	+1.57	25.6	11.6	+14.0
48	Ig α-1 chain isoform	P01876	6.35	6.08	+0.27	21.8	37.6	−15.8
49	Ig κ chain C isoform	P01834	6.35	5.58	+0.77	25.4	11.6	+13.8
51	Ig α-1 chain isoform	P01876	5.95	6.08	−0.13	21.8	37.6	−15.8
54	secretory actin-binding protein	P12273	4.94	5.47	−0.53	19.9	13.5	+6.4
55	cystatin D	P28325	5.98	6.76	−0.78	15.5	13.9	+1.6
56	Zn-α-2-glycoprotein	P25311	5.46	5.58	−0.12	49.9	32.1	+17.8
57	Zn-α-2-glycoprotein	P25311	5.32	5.58	+0.26	50.0	32.1	+17.9
60	poly Ig receptor	P01833	6.13	5.59	+0.54	107.4	81.4	+26.0
61	histatin 3	P15516	10.15	9.99	+0.16	9.8	4.1	+5.7
62	Ig κ chain C isoform	P01834	7.56	5.58	+1.98	29.3	11.6	+17.7
65	lysozyme C	P00695	9.20	9.28	−0.08	16.4	14.7	+1.7
72	histatin 6	P15516	11.31	11.05	−0.26	9.2	3.2	+6.0
80	PRG or G1 proline rich glycoprotein	NP_006240	11.26	11.35	−0.09	86.2	35.1	+51.1
92	serum albumin	P02768	6.12	5.67	+0.45	89.0	66.5	+22.5

Peptide Synthesis. Peptides with the sequences GQPQGPPRPPQGGRPSRPPQ and HHGYKRKF were custom synthesized by Genemed Synthesis, Inc. Peptides were purified by reversed phase HPLC, and their molecular weight was confirmed by MALDI TOF MS.

Candidacidal Activity Assay. A single colony of *Candida albicans* SC5345 was grown overnight, then diluted to an OD_{600} of 0.1 in 10 mL of 1% yeast extract/2% Bactopeptone/1% dextrose (YEPD) and grown exponentially at 25 °C to an OD of 1.0. Next the cells were centrifuged, washed twice with distilled water, and resuspended at a concentration of 10^6/mL in 20 mM sodium phosphate, pH 7.4. Five-microliter aliquots of the cell suspension were incubated with an equal volume of peptide (GQPQGPPRPPQGGRPSRPPQ, HHGYKRKF; 0−200 μM) at 37 °C for 3 h, after which the cells were plated on YEPD/agar and incubated overnight at 37 °C. The survival rate was calculated as a percentage: number of colonies recovered from treated cells/number of colonies from control cells. The effect of each peptide concentration was analyzed in triplicate. *Candida* cells incubated with or without 200 μM peptide were stained with the vital dye phloxine B, which stains dead cells, and examined 10−30 min after treatment (*63*). Microscopic images were acquired on a Leica DM5000 fluorescence microscope equipped with a Leica DFC480 digital camera.

RESULTS

2D SDS−PAGE of Human Parotid Saliva. The results of experiments in which human parotid proteins from a single individual, concentrated by ultrafiltration, were separated by 2D SDS−PAGE are shown in Figure 1. Essentially the same results were obtained when the samples were prepared by acetone precipitation (data not shown). Figure 1A shows a typical 2D gradient gel (∼pH 3−10) separation of parotid proteins, which are numbered. The high p*I* range contained many clustered spots that were better resolved when the sample was separated on a gel with a narrower isoelectric focusing range (∼pH 6−11; Figure 1B). Several of the newly resolved proteins likely belong to the PRP family, as judged by the pink color that was generated when the gel was stained with Coomassie blue R250.

MS Identification of Protein Spots. Individual proteins that were identified in MS experiments are listed in Table 1. MALDI TOF MS and oMALDI QqTOF MS/MS data that were used for identification of a subset of the numbered spots are summarized in Table 2. In general, the PMF data, which covered a large portion of the sequence, were the primary protein identification tools. In most cases, MS/MS data were also obtained. To further increase our confidence in the results, we compared the experimentally observed protein isoelectric points and molecular weights with their theoretical values (Table 1), which, with a few exceptions (such as α-amylase, discussed below), were in good agreement. Known constituents of parotid saliva that were identified in spots obtained from ∼pH 3−10 gradient gels included histatin 1, cystatin SA, cystatin B, cystatin D, carbonic anhydrase VI, acidic proline-rich phosphoproteins, secretory immunoglobulin A, Ig κ chain, and IgA α-chain. Proteins that appeared in the most basic region of ∼pH 6−11 gels included histatin 3 (spot 61), lysozyme C (spot 65), and the proline-rich glycoprotein (PRG) (spot 80). The same spots and proteins, as determined by MS analyses, were present in the parotid saliva samples of two additional individuals.

We also detected in all three saliva samples novel proteins not known to be constituents of parotid saliva: secretory actin-binding protein (or prolactin-inducible protein), cystatin B, and Zn-α-2-glycoprotein. Figure 2 is a comparison of the 2D SDS−PAGE regions of the individual samples that

Table 2: Summary of MALDI TOF MS, oMALDI QqTOF MS/MS, and MALDI TOF/TOF MS/MS Data on Which Protein Identification Was Based[a]

spot ID	protein identified	sequence coverage (%)	experimental monoisotopic $[MH]^+$ of matched peptides (position)
5	poly Ig receptor	31.2	812.4 (53−57)[1], 903.5 (289−296)[1], 1044.5 (480−487), 1079.5 (147−155), 1211.5 (516−525), 1250.7 (305−316), 1370.6 (537−547), 1402.7 (395−406), 1539.7 (623−638) or (383−394), 1549.8 (361−375), 1657.8 (62−77), **1856.9 (251−268)**, 1988.9 (498−515), 2008.9 (548−565)[q], 2026.0 (548−565), 2042.9 (212−230), 2181.0 (212−231)[1]
13	serum albumin	17.6	**927.5 (162−168)**, 960.6 (427−434), 973.5 (29−36)[1], 1074.5 (206−214)[1], 1149.6 (25−34)[1] or (66−75), 1226.6 (35−44)[1], 1358.7 (570−581)[Ox], 1627.7 (585−598)[2], 1640.0 (438−452)[1], 1657.8 (414−426)
16	Zn-α-2-glycoprotein	45.0	926.5 (232−238), 1127.6 (239−248), 1233.5 (222−231), **1276.6 (165−174)**, 1368.7 (89−99)[1,Ox] 1408.7 (25−36), **1451.7 (177−188)**, 1515.8 (163−174)[q,1], 1532.8 (163−174)[1], 1717.8 (134−146)[1], 1758.9 (201−217)[q], 2403.2 (37−57)
18	carbonic anhydrase VI	27.1	918.4 (258−264), 938.5 (47−54)[q], 955.5 (47−54), 1074.5 (258−265)[1], 1096.6 (247−255), 1163.6 (296−304), 1575.8 (194−207)[Ox], 2776.4 (273−295)
23	carbonic anhydrase VI	41.6	865.4 (266−272), 918.4 (258−264), 938.5 (47−54)[q], 955.5 (47−54), 1074.5 (258−265)[1], 1096.6 (247−255), **1163.6 (296−304)**, 1575.8 (194−207)[Ox], 1588.9 (133−145), **2292.2 (148−169)**, 2776.3 (273−295)
26	histatin 1	86.8	825.4 (26−31)[1] or (25−30)[1], 1214.6 (33−41)[1], 1342.7 (32−41)[2], 1494.8 (26−36)[3], 1498.8 (31−41)[2], **1963.8 (42−57)**
28	cystatin B	55.1	924.4 (92−98), 1123.5 (90−98)[1], 1326.7 (45−56), **1422.7 (57−68)**, 2458.3 (69−89)
29	histatin 1	86.8	825.4 (26−31)[1] or (25−30)[1], 1214.6 (33−41)[1],1342.7 (32−41)[2], 1498.8 (31−41)[2], 1963.8 (42−57)
36	cystatin SA	76.6	1692.9 (29−43), 2076.1 (29−46)[1], 2077.1 (29−46)[1,d], 1320.8 (47−57), 2349.2 (47−65)[1,d], 1202.6 (58−66)[1], 2169.2 (73−91)[1], 1924.0 (75−91)[q], 1942.0 (75−91), 2142.1 (97−114), 2143.1 (97−114)[d], 2270.2 (97−115)[1], 2271.2 (97−115)[1,d], 2098.1 (115−130)[1], 2114.1 (115−130)[Ox], 1953.0 (116−130)[q], 1969.0 (116−130)[q,Ox], 1970.0 (116−130), 1971.0 (116−130)[d], 1986.0 (116−130)[Ox]
41	PRP-C acidic proline-rich phosphoprotein	50.7	**1605.8 (108−122)[1]**, **1731.9 (91−107)**, 2092.0 (146−166)[1], 2296.2 (123−145)[1], 3054.6 (125−155)[1], 3267.8 (123−155)[2]
42	PRP-C acidic proline-rich phosphoprotein	50.7	**1605.8 (108−122)[1]**, **1731.9 (91−107)**, 2092.1 (146−166)[1], 2296.2 (123−145)[1], 3054.5 (125−155)[1], 3267.7 (123−155)[2]
43	PRP-C acidic proline-rich phosphoprotein	50.7	1120.5 (156−166), 1605.8 (108−122)1, 1731.9 (91−107), 2092.1 (146−166)[1], 2296.2 (123−145)[1], 3054.5 (125−155)[1], 3267.7 (123−155)[2]
46	Ig κ chain C isoform	74.5	869.4 (100−106)[1], 1797.9 (19−34), **1875.9 (83−99)**, 1946.0 (1−18), 2136.0 (42−61)
48	Ig α-1 chain C isoform	19.0	896.4 (276−282),**1213.6 (264−273)**, 1375.5 (201−212), 1818.8 (283−299)[q], **1835.8 (283−299)**, 2352.9 (307−327)[Ox]
49	Ig κ chain C isoform	67.9	1797.9 (19−34), 1875.9 (83−99), **1946.0 (1−18)**, 2136.0 (42−61)
51	Ig α-1 chain C	11.0	**1213.6 (264−273)**, 1375.6 (201−212), 1818.8 (283−299)[q], 1835.8 (283−299)
54	secretory actin-binding protein	71.2	1026.6 (137−144), 1283.8 (107−118), **1356.5 (86−96)**, 1610.8 (119−133), 1814.9 (70−85), 1995.0 (119−136)[1], 2069.1 (45−63)
55	cystatin D	57.4	850.5 (132−138), 1425.7 (29−42), 1744.8 (43−57), **1773.7 (98−112)**, 2427.1 (113−131)[1]
56	Zn-α-2-glycoprotein	55.0	926.5 (232−238), 974.5 (65−72), 1102.6 (64−72)[1], 1127.6 (239−248), 1276.6 (165−174), 1352.7 (89−99)[1], 1368.7 (89−99)[1,Ox], 1451.7 (177−188), 1475.7 (165−176)[1], 1515.8 (163−174)[q,1], 1532.8 (163−174)[1], 1579.8 (177−189)[1], 1717.8 (134−146)[1], 1758.9 (201−217)[q], 1775.9 (201−217), 1782.9 (147−162), 2387.2 (196−217)[1], 2403.2 (37−57)
57	Zn-α-2-glycoprotein	47.1	808.4 (134−139), 926.5 (232−238), 974.5 (65−72), 1125.5 (91−99), 1127.6 (239−248), 1233.6 (222−231), 1276.6 (165−174), 1352.7 (89−99)[1], 1368.7 (89−99)[1,Ox], 1408.7 (25−36), 1451.7 (177−188), 1475.7 (165−176)[1], 1515.8 (163−174)[q,1], 1532.8 (163−174)[1], 1579.8 (177−189)[1], 1717.8 (134−146)[1], 1775.9 (201−217), 1948.9 (73−88)[1], 1964.9 (73−88)[1,Ox]
60	poly Ig receptor	34.6	903.5 (289−296)[1], 1211.5 (516−525), 1224.6 (53−61)[1], 1250.7 (305−316), 1370.6 (537−547), 1402.7 (395−406), 1539.7 (623−638) or (383−394), 1549.8 (361−375), 1572.7 (713−726), 1857.0 (251−268), 1974.9 (435−450), 2009.0 (548−565)[q], 2026.0 (548−565), 2043.0 (212−230), 2114.2 (193−211), 2172.2 (297−316)[1], 2241.2 (232−250), 2300.3 (297−317)[2], 2383.4 (191−211)[1], 3299.6 (20−49)
65	lysozyme C	22.3	**1012.5 (52−59)**; 1039.6 (117−125)[1], **1400.7 (69−80)**
72	histatin 6	100	1342.7 (12−21)[2], 1498.8 (11−21)[3], 1718.9 (12−24)[3], 2121.1 (6−21)[4], 2277.2 (5−21)[5], 2497.3 (6−24)[5], 2625.3 (4−23)[6], 2653.3 (5−24)[6], 2815.4 (1−21) 2871.4 (1−22)[7], 3035.5 (1−23)[7], 3191.6 (1−24)[7]
80	PRG	13.7	**2536.1 (17−39)[q,p,1]**, **2438.1 (17−39)[q,dh,1]**, **1213.6 (28−39)[1]**, **2404.2 (287−309)[2]**
92	serum albumin	33.5	927.5 (162−168), 960.6 (427−434), 1149.6 (25−34)[1] or (66−75), 1226.6 (35−44)[1], 1358.7 (570−581)[Ox], 1623.8 (362−375), 1639.9 (438−452)[1], 1657.8 (414−426), 1714.9 (118−130)[1], 1899.1 (169−183)[1] or (170−184)[1], 1911.0 (509−524), 1932.1 (89−105)[1], 1997.0 (123−138)[1], 2045.1 (397−413), 2260.1 (525−543), 2545.2 (525−545)[1]

[a] Key to symbols: ([d]) deamidation of Q or N; ([q]) N-terminal pyro-glutamine; ([p]) phosphorylation; ([dh]) dehydroalanine; ([1]) one missed cleavage site; ([2]) two missed cleavage sites; ([3]) three missed cleavage sites; ([Ox]) oxidation of methionine. Bold type indicates peptide identity verified by MS/MS. Calculation of sequence coverage and amino acid residue numbering were based on theoretical sequences without signal peptides.

contained two of these novel proteins. Portions of the mass spectra that led to the identification of these components are shown in Figure 3. MALDI TOF MS analysis of protein spot 16 showed numerous peptide ions that correspond to amino

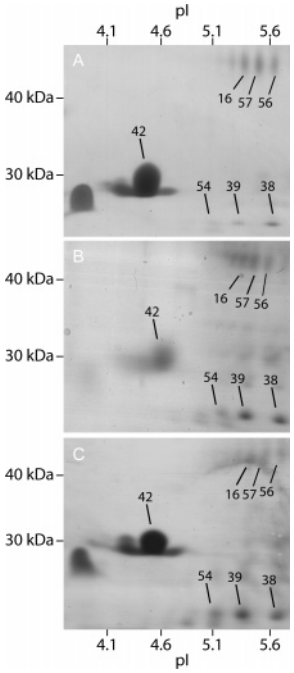

FIGURE 2: Comparison of the 2D SDS−PAGE regions of samples from three individual donors (panels A−C) that contained several of the novel components identified in this study. Specifically, spots 16, 56, and 57 were identified as Zn-α-2-glycoprotein, spot 54 was identified as secretory actin-binding protein, and spots 39 and 38 were identified as fragments of α-amylase. Spot 42 corresponded to PRP C.

acid sequences, numbered according to their position along the peptide backbone of the Zn-α-2-glycoprotein (Figure 3A). We used MS/MS to confirm the sequence of several of these trypsin cleavage products. For example, Figure 3B shows the MS/MS spectrum of peptide AYLEEECPATLR ($[MH]^+$ *m*/*z* 1451.7) corresponding to amino acid residues 177−188 of Zn-α-2-glycoprotein. The majority of peptide bond cleavages were observed, as indicated by y- and b-series ions. Figure 3C shows a MALDI TOF/TOF MS/MS spectrum of peptide VHVGDEDFVHLR ($[MH]^+$ *m*/*z* 1422.7; amino acids 57−68) confirming the presence of cystatin B in spot 28.

Posttranslational modifications (glycosylation, phosphorylation, or proteolytic processing) are likely explanations for the presence of electrophoretically distinguishable isoforms of parotid proteins. For example, differences in oligosaccharide chain length and composition probably account for some of the numerous α-amylase spots in the 50- to 76-kDa region of the gel, a possibility that was previously suggested (*64*). We were surprised by the number of protein isoforms with estimated molecular weights that were much lower than that of the full-length form of α-amylase (data tabulated in the Supporting Information). A nearly identical pattern of α-amylase fragments was found among the three donors (for example spots 38 and 39 in Figure 2), as well as in previous studies of whole saliva (*16*, *17*). Together, these results suggest that the amylase products were generated by a discrete mechanism rather than by random proteolysis. This observation suggests that saliva contains substantial amounts of cleaved (or splice variant) forms of certain proteins. The same conclusion is further substantiated by our analysis of the ≤10-kDa fraction of parotid saliva (discussed below).

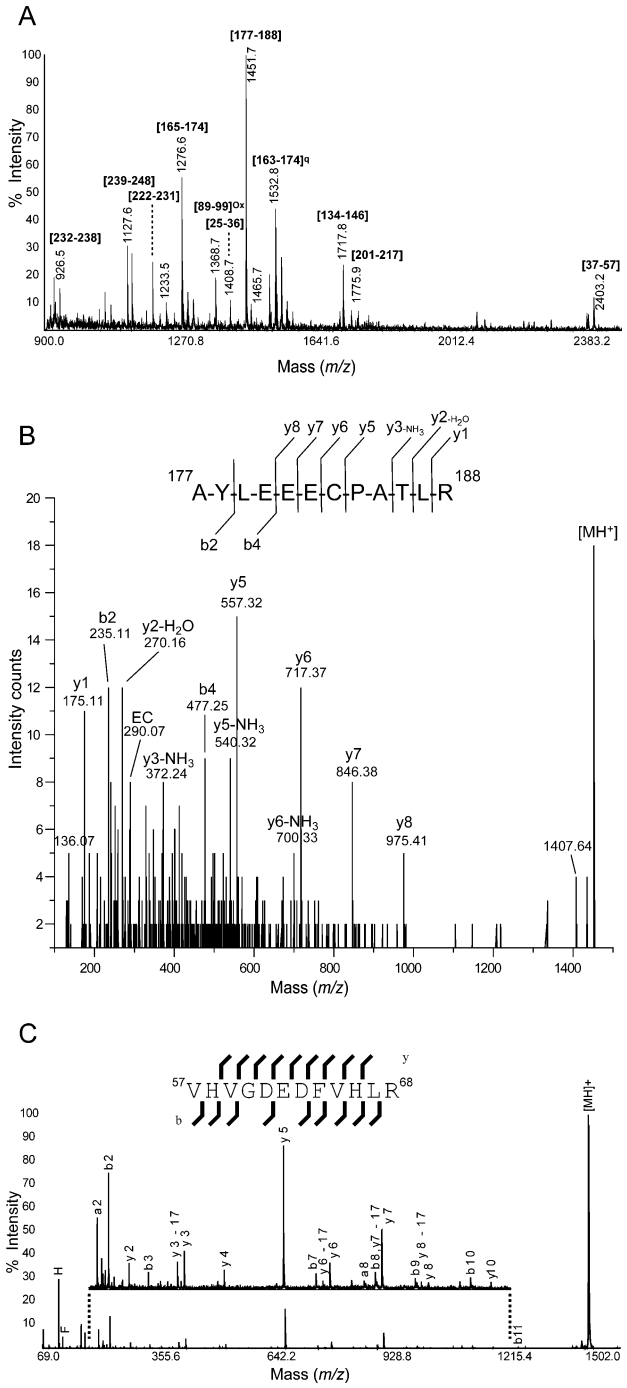

FIGURE 3: (A) MALDI TOF MS PMF of spot 16 (see Figure 1A). Peaks matching Zn-α-2-glycoprotein tryptic fragments are labeled with their N- and C-terminal amino acid residues in parentheses. (B) Annotated MS/MS spectrum of tryptic peptide AYLEEEC-PATLR ($[MH]^+$ *m*/*z* 1451.7), corresponding to amino acid residues 177−188 of Zn-α-2-glycoprotein, confirming the identity of spot 16. (C) MALDI TOF/TOF MS/MS analysis of the tryptic peptide VHVGDEDFVHLR ($[MH]^+$ *m*/*z* 1442.7) corresponding to amino acid residues 57−68 of cystatin B, confirming the identity of spot 28 (Figure 1A). Superscript Q: pyro-glutamination. Superscript Ox: methionine oxidation.

Detection of a Novel Phosphorylation Site on the PRG. The MALDI TOF mass spectrum of spot 80, the PRG, contained two prominent metastable ions that may indicate phosphorylation (Figure 4A). These ions were observed at *m*/*z* of approximately 80 and 98 Da less than the value corresponding to the tryptic peptide, pyroQ^{18}SLNEDV^{24}-

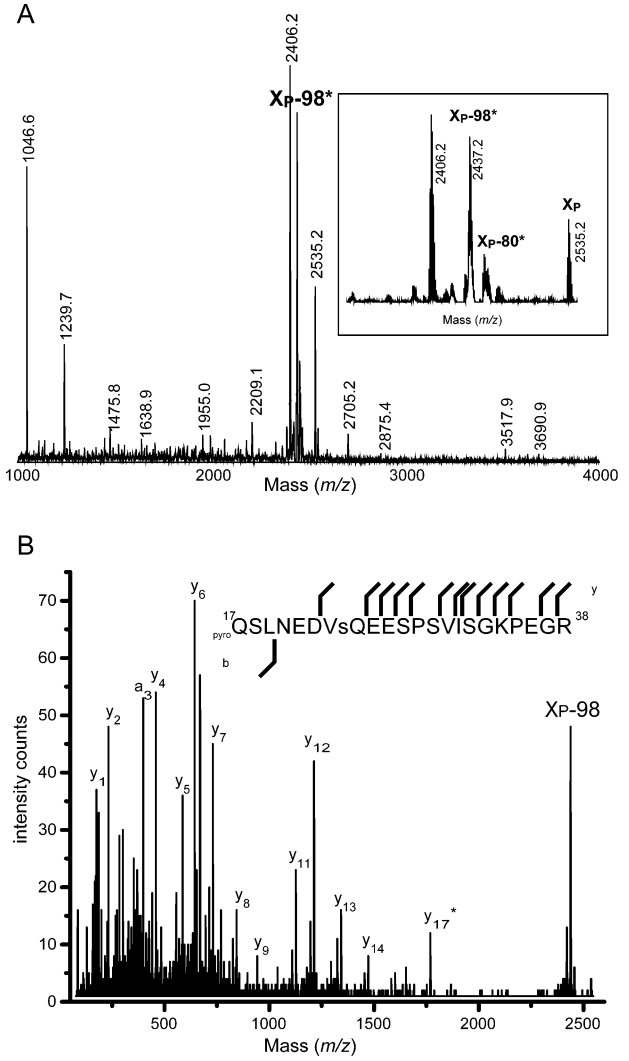

FIGURE 4: Identification of a novel phosphorylation site on the PRG. (A) MALDI TOF mass spectrum of peptides obtained by tryptic digestion of protein spot 80 (Figure 1B). The inset shows the phosphorylated peptide Xp (*m*/*z* 2535.2) and the metastable ions Xp-80* and Xp-98* derived in the process of post-source decay. The protein was identified by matching MS/MS fragmentation data of peptide molecular ions $[MH]^+$ *m*/*z* 1239.7 and *m*/*z* 2406.2 to PRG (NCBI accession number: NP_006240). (B) Confirmation of Ser24 as a novel phosphorylation site on the PRG. MS/MS spectrum of tryptic phosphopeptide Xp ($[MH]^+$ *m*/*z* 2535.2) corresponding to residues 17−39 (pyroQSLNEDVsQEESPSVISGKPEGR) of the PRG. Phosphorylation is indicated by a strong ion [Xp-98] generated by neutral loss of phosphate from the precursor ion.

sQEE[28]SP[30]SVI[33]SGKPEGR ($[MH]^+$ *m*/*z* 2535.2, residues 17−39), suggesting the neutral loss of H_3PO_4 and H_3PO_3 in the process of post-source decay (*65*, *66*). In a tandem MS spectrum of this peptide, the y17 fragment, indicative of dehydroalanine formation at Ser24, was observed (Figure 4B). Observation of the y7−y14 fragment ions suggested that Ser28, Ser30, and Ser33 within the sequence EESPSVIS are not phosphorylated. In addition, the presence of a strong a3 ion indicated that Ser18 is not phosphorylated. Taken together, these data suggest that Ser24 of the PRG is phosphorylated. Interestingly, this site has a strong score for possible phosphorylation (0.997) as predicted by the NetPhos 2.0 algorithm (*67*).

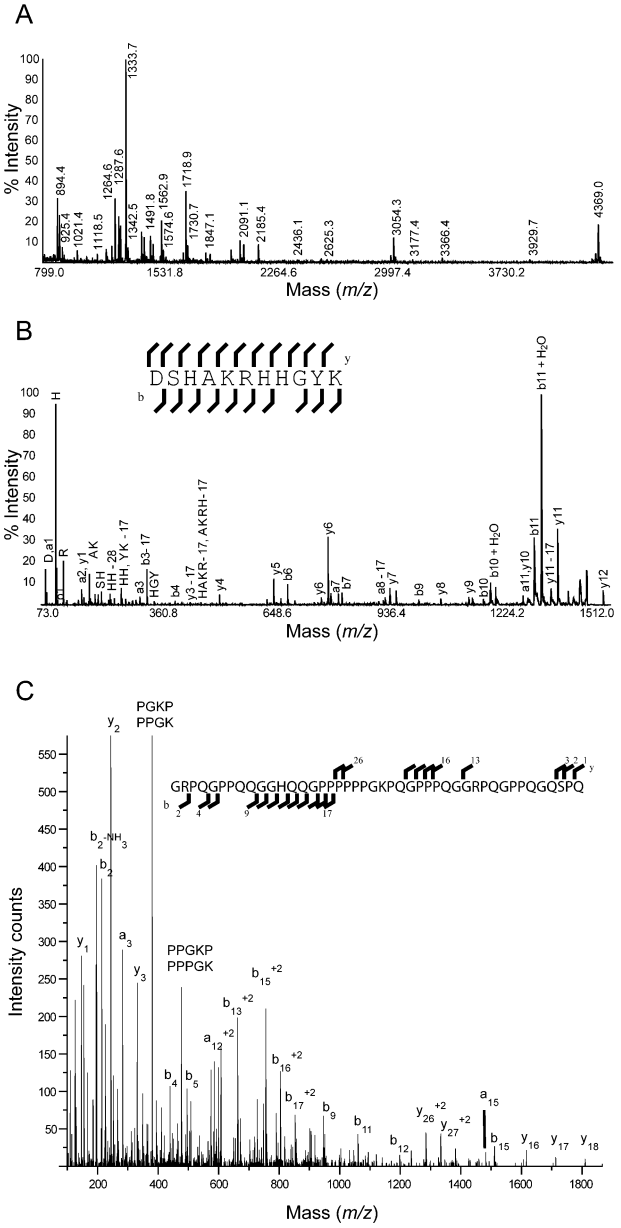

FIGURE 5: The low-molecular-weight fraction of human parotid saliva contains numerous peptides. (A) MALDI TOF MS analysis of the ≤10-kDa fraction obtained by ultrafiltration. (B) MALDI TOF/TOF MS/MS analysis of the N-terminal histatin peptide, DSHAKRHHGYK $[MH]^+$ *m*/*z* 1491.8. (C) MS/MS spectrum of peptide P-C, a portion of the salivary acidic proline-rich phosphoprotein (Swiss-Prot accession number P02810).

MS Analysis of the ≤10-kDa Fraction of Parotid Saliva. From the initial MALDI TOF MS spectra of parotid saliva it was apparent that the ≤10-kDa fraction was rich in peptide components, a phenomenon that was previously reported (*42*, *43*, *46*). The same peptide repertoire was observed when the samples were collected into a proteinase inhibitor cocktail, formic acid or trifluoroacetic acid, suggesting that the peptides are formed prior to or during the secretion process rather than by subsequent in vitro degradation. This conclusion was further supported by our analysis of the low-molecular-weight components of a saliva sample from a different donor that produced similar results (data not shown).

Interestingly, the majority of peptides we detected were not derived from the most abundant parotid proteins, but rather were the cleavage products of PRP and histatin protein

Table 3: Subset of Peptides Identified in the ≤10-kDa Fraction of Human Parotid Saliva[a]

[MH]$^+$	precursor protein	Swiss-Prot accession no.	position		sequence
894.5	PRP-1 or PRP-2	P04280/P02812	[324−331]	*	(*PPQG*) *GRP*SRPPQ ( )
1273.7	PRP-1	P04280	[320−331]	*	(R) *PPQGGRP*SRPPQ ( )
1276.6	PRP-C	P02810	[155−166]	*	(*PPQGG) RP*QGPPQGQSPQ ( )
1315.7	peptide P-A	P02814	[55−67]	*	(Y) GPGRIPPPPPAPY (G)
1333.7	PRP-C	P02810	[154−166]	*	(*PPQG*) *GRP*QGPPQGQSPQ ( )
1421.7	histatin 1	P15515	[20−30]		( ) DSHEKRHHGYR (R)
1443.6	histatin 1	P15515	[46−57]	*	(F) YGDYGSNYLYDN ( )
1471.7	peptide P-C	P02810	[123−136]		(R) GRPQGPPQQGGHQQ (G)
1758.8	histatin 1	P15515	[20−32]	*	( ) DsHEKRHHGYRRK (F)
1761.9	PRP-C	P02810	[107−122]	*	(G) RPQGPPQQGGHPRPPR (G)
1866.9	peptide P-C (IB-8b)	P02810	[148−166]	*	(Q) GPPPQGGRPQGPPQGQSPQ ( )
2091.1	PRP-2	P02812	[232−251]	*	(A) GQPQGPPR*PPQGGRP*SRPPQ ( )
2186.2	BAT-3	P46379	[616−641]	*	(L) GPAGPGAGGPGVASPTITVAMPGVPA (F)
4369.2	peptide P-C (IB-8b)	P02810	[123−166]		(R) GRPQGPPQQGGHQQGPPPPPPGKPQGP*P PQGGRP*QGPPQGQSPQ ( )

[a] Peptides were analyzed by MS/MS before and after reversed phase nano-HPLC separation. In some instances, identities were derived by using a combination of approaches, including de novo interpretation of MS/MS data. The italicized amino acid sequence *PPQG/GRP* refers to a possible consensus site for an unknown salivary proteinase. Novel peptides are indicated by an asterisk.

family members. Figure 5A shows a typical MALDI TOF MS spectrum of the ≤10-kDa fraction after passage through a C18 ZipTip. Somewhat surprisingly, numerous ions were easily resolved. Subsequently, the majority of the peptides in this fraction were subjected to MS/MS analyses with interesting results. For example, 14 fragments of PRPs and histatin 1 were detected (Table 3), 11 of which are seemingly novel. Fragments of histatin 3 were very abundant and are summarized separately in Table 4 and in Figure 6, which illustrates the possible processing of the precursor molecule. Some of these peptides have been described [e.g., histatin 7 (*68*)], but others are novel. Figure 5B shows a representative MALDI TOF/TOF MS/MS spectrum of one of the peptides, DSHAKRHHGYK ([MH]$^+$ *m*/*z* 1491.8), which corresponds to the N-terminal portion of histatin 3. Identifying the source of other peptides in the low-molecular-weight fraction was more difficult due to the presence of multiple proline residues within the sequences. Figure 5C shows the MS/MS spectrum of peptide P-C from the salivary acidic proline-rich phosphoprotein (Swiss-Prot accession no. P02810). Fragment ion formation was primarily driven by the proline residues. As often observed for proline-containing peptides, internal product ions (products of two peptide bond cleavages) are abundant (e.g., PGKP, PPGK). Table 4 summarizes the histatin 3-derived peptides identified in this study. Overall, 60 peptides were found, 50 of which were confirmed by MS/MS analyses; 10 were putatively assigned sequences based on their molecular masses. As shown in Table 4, 25 of the 50 validated peptides were, to the best of our knowledge, novel. In the other cases, published studies are cited in the table, and antifungal activity is noted where applicable.

Finally, we mapped each peptide back to its parent molecule, as shown in Figure 6 for histatin 3, the major source of protein fragments in this fraction. For this purpose we used a combination of the data generated in this study and published peptide sequences. Color coding illustrates potential proteolytic cleavage sites. Many of the observed peptides were likely derived by tryptic or chymotryptic-like processing of common precursor polypeptides, whereas other products were indicative of different proteinase activities.

Evaluating Candidacidal Activity of Individual Peptides. Next, we sought insights into the biological relevance of the salivary peptides. Toward this end we synthesized peptide analogues of one PRP fragment and one histatin fragment and tested their antifungal properties. Peptide GQPQGPPRPPQGGRPSRPPQ had no discernible effects, but peptide HHGYKRKF showed dose-dependent candidacidal activity (Figure 7A). To understand more about the mechanisms involved, we stained *C. albicans* cells that were incubated with this peptide (200 μM) with the vital dye phloxine B. The microscopic images (Figure 7B−I) showed rapid staining of dead and dying cells, with large aggregates of cytoplasmic material spilling out of the cells. The cytotoxic effect was shown for the yeast as well as the germ tube/early hyphal form of *C. albicans*. To the best of our knowledge, HHGYKRKF is the shortest histatin peptide with candidacidal activity reported to date.

DISCUSSION

By using conventional (e.g., 2D SDS−PAGE) and relatively unconventional (e.g., ultrafiltration) separation approaches, coupled with MS identification of the products, we obtained complementary views of the human parotid saliva proteome. The results revealed novel components as well as a surprising number of isoforms and fragments. 2D SDS−PAGE allowed the visual identification of protein isoforms that were likely generated by posttranslational modifications (glycosylation, phosphorylation, or proteolytic processing), for example, the characteristic clustering of α-amylase spots in the 50- to 76-kDa region. We note that it is usually very difficult to ascertain the presence of multiple protein isoforms solely on the basis of MS data. Additionally, 2D SDS−PAGE analyses can give other clues about protein identity. In this case, staining with Coomassie blue R250 revealed PRPs as pink rather than blue spots. As noted by Costello and co-workers (*69*), members of this family are challenging to identify by MS/MS owing to the high efficiency of collision-induced dissociation at the amide bond N terminal to proline residues. This phenomenon results in a low relative abundance of fragment ions arising from cleavages at other amide bonds. Despite the aforementioned advantages, SDS−PAGE typically excludes the low-molecular-weight proteome. To avoid this problem we introduced an ultrafiltration step in conjunction with LC-MALDI analyses. The molecular weight cutoff we used (≤10000) led to the inclusion of a subset of peptides in samples

Table 4: Experimentally Observed Histatin 3 Peptides and Their Antifungal Activities[a]

sequence	[MH$^+$]	this study	novel	start	end	name	anti-fungal act.	refs
(H) HSHRGY (R)	756.4	X		38	43			*42−44*
(S) NYLYDN ( )**	801.3	X		46**	51**			*42*, *43*
( ) DSHAKRH (H)	850.4	X	*	20	26			
(K) HHSHRGY (R)	893.4	X		37	43	HRP-3f		*43*
(R) HHGYKRK (F)	925.5	X		26	32			*43*
(A) KRHHGYK (R)	925.5	?		24	30	histatin 12		*40*, *43*
(H) EKHHSHR (G)**	929.5	X	*	35**	41**			
(H) HGYKRKF (H)	935.6	X	*	27	33			
( ) DSHAKRHH (G)	987.5	X		20	27	N		*103*
(E) KHHSHRGY (R)	1021.5	X		36	43			*104*
(Y) RSNYLYDN ( )	1044.5	X		44	51	C	0	*103*
(K) HHSHRGYR (S)	1049.6	X	*	37	44			
(F) HEKHHSHR (G)**	1067.6	X	*	34**	41**			
(R) HHGYKRKF (H)	1072.6	X	*	26	33		++	
(A) KRHHGYKR (K)	1081.6	X		24	31	histatin 11, HRP-6d		*40*, *43*, *44*
(F) HEKHHSHRG (Y)	1124.5	X	*	34	42			
(H) EKHHSHRGY (R)	1150.6	X	*	35	43			
(G) YRSNYLYDN ( )	1207.5	X	*	43	51			
( ) DSHAKRHHGY (K)	1207.6	X	*	20	29			
(A) KRHHGYKRK (F)	1209.6	X		24	32			*43*
(K) FHEKHHSHR (G)**	1214.6	X		33**	41**	HRP-5e or 4d		*44*
(R) GYRSNYLYDN ( )	1264.6	X	*	42	51			
(K) FHEKHHSHRG (Y)	1271.7	X	*	33	42			
(F) HEKHHSHRGY (R)	1287.6	X		34	43	HRP-6b, C10	+	*42−44*, *105*
(H) ^{Q}EKHHSHRGYR (S) pyroglu	1288.7	X	*	35^{q}	44			
(H) EKHHSHRGYR (S)	1306.6	X	*	35	44			
( ) DSHAKRHHGYK (R)	1335.7	X		20	30	HRP-3e	++	*43*, *44*
(H) RGYRSNYLYDN ( )	1420.7	X	*	41	51			
(K) FHEKHHSHRGY (R)	1434.7	X		33	43			*43*
(F) HEKHHSHRGYR (S)	1443.7	X		34	44	HRP-5c		*43*, *44*
( ) DSHAKRHHGYKR (K)	1491.8	X		20	31	P-112	0/+	*43*, *106*
(S) HRGYRSNYLYDN ( )	1557.7	X	*	40	51			
(R) KFHEKHHSHRGY (R)	1562.8	X		32	43	histatin 8, C12, P116	+; 0/+	*40*, *43*, *44*, *105*, *106*
(K) FHEKHHSHRGYR (S)	1590.8	X		33	44			*43*
(R) HHGYKRKFHEKH (H)	1603.8	X		26	37	P-114	0/+	*106*
( ) DSHAKRHHGYKRK (F)	1619.9	X		20	32	HRP-5d		*43*, *44*
(H) SHRGYRSNYLYDN ( )	1644.7	X	*	39	51			
(K) RKFHEKHHSHRGY (R)	1718.9	X		31	43	histatin 7, HRP-6a, Pba	+	*40*, *43*, *44*
(R) KFHEKHHSHRGYR (S)	1718.9	X		32	44	histatin 10, HRP-4b		*40*, *43*, *44*
(Y) KRKFHEKHHSHRGY (R)	1847.0	X		30	43	C14	++	*105*
(K) RKFHEKHHSHRGYR (S)	1875.0	#		31	44	histatin 9, HRP-4b	+	*40*, *44*, *106*
(R) HHGYKRKFHEKHHSH (R)	1964.8	X	*	26	40			
(A) KRHHGYKRKFHEKHH (S)	2025.1	X	*	24	38			
( ) DSHAKRHHGYKRKFHE (K)	2033.0	#		20	35	N16	+	*105*
(H) GYKRKFHEKHHSHRGY ( )	2067.1	#		28	43	C16, Hst M	++	*103*, *105*
(R) HHGYKRKFHEKHHSHR (G)	2121.1	X	*	26	41			
( ) DSHAKRHHGYKRKFHEK (H)	2161.1	#		20	36	HRP-5b		*44*
(H) EKHHSHRGYRSNYLYDN ( )	2177.0	X	*	35	51			
(F) HEKHHSHRGYRSNYLYDN ( )	2313.1	X	*	34	51			
(R) HHGYKRKFHEKHHSHRGY (R)	2341.2	#		26	44			*44*
( ) DSHAKRHHGYKRKFHEKHH (S)	2435.1	X	*	20	38			
(K) FHEKHHSHRGYRSNYLYDN ( )	2461.2	X	*	33	51			
(K) RHHGYKRKFHEKHHSHRGY (R)	2497.3	#		25	43	HRP-5a		*44*
(R) KFHEKHHSHRGYRSNYLYDN ( )	2588.2	X	*	32	51			
(A) KRHHGYKRKFHEKHHSHRGY (R)	2625.3	X		24	43	HRP-6	0/+	*44*
(K) RKFHEKHHSHRGYRSNYLYDN ( )	2744.3	X		31	51	histatin 4, HRP-3a, Pbe	+/++	*40*, *44*
( ) DSHAKRHHGYKRKFHEKHHSHR (G)	2815.4	#		20	41	HRP-3c		*44*
( ) DSHAKRHHGYKRKFHEKHHSHRGY (R)	3035.5	X		20	43	histatin 5, Pbd	++	*40*, *43*, *44*, *68*
( ) DSHAKRHHGYKRKFHEKHHSHRGYR (S)	3191.6	#		20	44	histatin 6, HRP-3b, Pbb		*40*, *43*, *44*
( ) DSHAKRHHGYKRKFHEKHHSHRGYRSNYLYDN ( )	4061.0	#		20	51	histatin 3		*40*, *43*, *44*

[a] Peptide sequences are shown with adjacent sequence residues and theoretical molecular weights [MH]$^+$. "Start" and "end" indicate the locations of the peptide sequence within the precursor protein. Peptides that could have been derived from either histatin 1 or 3 are indicated by double asterisks. Current nomenclature of peptides is indicated, as well as references for previously observed peptides. Histatins 1−7 are synonymous with HRP 1−7 (*38*, *107*). (^{q}) N-terminal pyro-glutamate. (#) Putative peptide identities based solely on their molecular masses. (*) Novel peptides. Reported relative antifungal activities are indicated by ++ and +, 0 representing no significant activity.

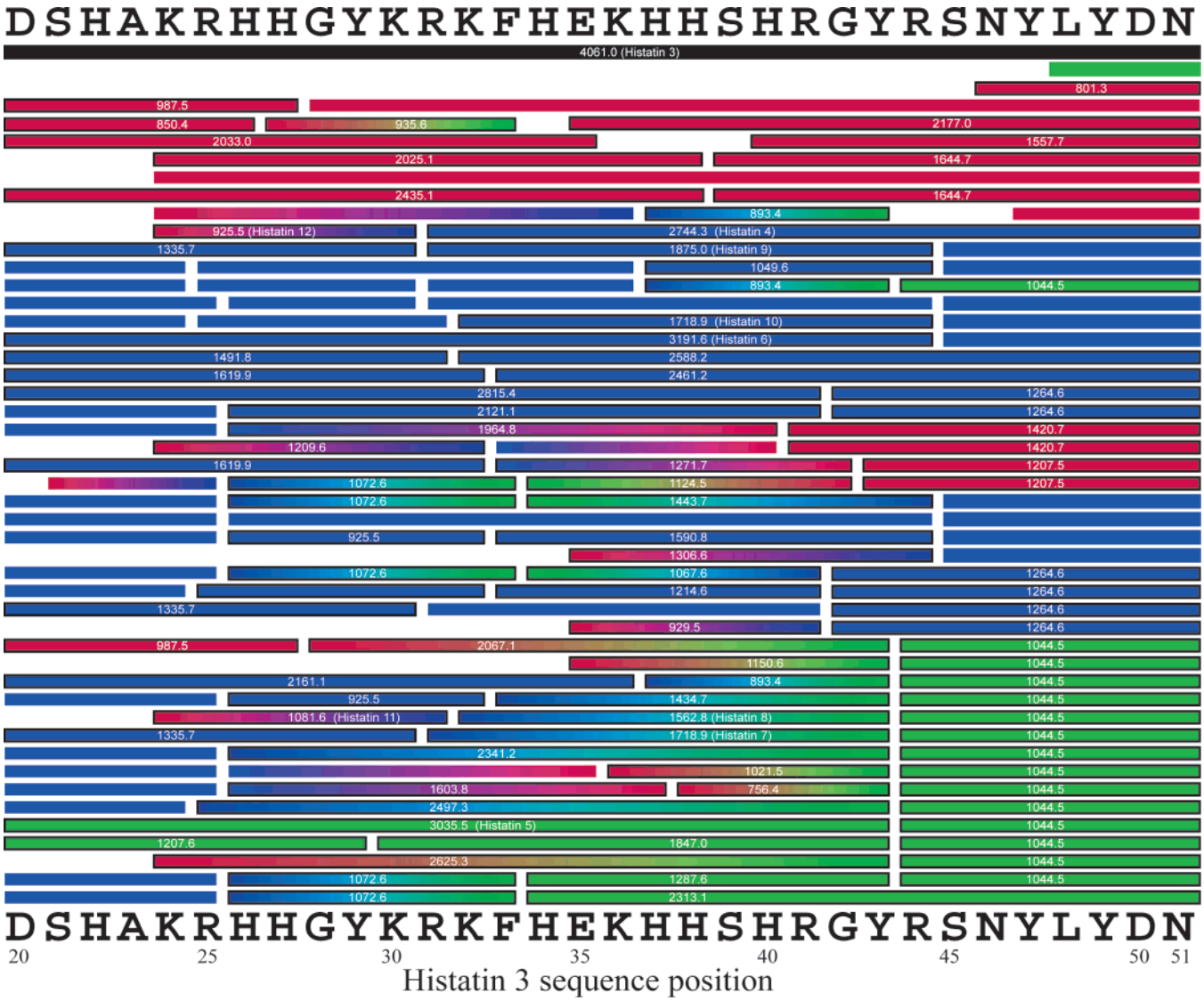

FIGURE 6: Summary of peptides derived from histatin 3, mapped back to the parent protein. Bars indicate the position and length of the peptides within the precursor sequence. A black border indicates that the respective peptide was experimentally observed in this study. The number within the bars corresponds to the respective $[MH]^+$. Bars without borders represent fragments reported in published studies. The color coding illustrates possible mechanisms of peptide generation: tryptic (blue), chymotryptic (green), or an unknown proteolytic activity (red). Feasible permutations are also shown.

produced by both separation techniques, e.g., histatins 3 and 6, providing us with additional evidence that we were capturing a significant portion of the salivary peptide repertoire.

The importance of analyzing each salivary gland secretion separately was illustrated by our discovery in parotid saliva of the secretory actin-binding protein (SABP), also known as the prolactin-inducible protein (PIP), gross cystic disease fluid protein (GCDFP-15), and glycoprotein 17 (GP17). As suggested by its multiple names, this protein has been detected in several body fluids, in particular, those that contain exocrine secretions including sweat, semen, and tears (*70*). Previous studies suggested that SABP, a component of whole saliva (*16*, *71*), was also found in the submandibular/sublingual fraction, which was thought to be the source. The apparent absence of this protein in parotid secretions is denoted by the name given to the salivary form of this molecule—the extraparotid glycoprotein (EP-GP) (*72*, *73*). Here, as part of our detailed analysis of the parotid salivary proteome, we detected several isoforms of SABP. Interestingly, this protein has functions that are relevant to oral health: a high affinity for hydroxyapatite (*72*) and the ability to bind bacteria (*73*, *74*), actin, fibronectin (*73*), and a CD4 receptor on monocytes (*75*). Recently, SABP was shown to have an aspartyl proteinase activity with narrow substrate specificity for gelatin and fibronectin (*76*).

In other cases we gained additional information about the origin of proteins that were already known to be salivary components. For example, we found in parotid saliva several isoforms of the Zn-α-2-glycoprotein, which has been detected in several human body fluids including whole saliva (*16*, *17*). The biological functions of this molecule, which are not completely understood, seem to involve lipid metabolism (*77*), and elevated levels in serum have been associated with prostate cancer (*78*). Our data are consistent with the results of immunohistochemical analyses that localized this glycoprotein to the serous cells of the parotid (and submandibular) gland (*79*). Likewise, we detected cystatins B and D in parotid saliva, thereby confirming the parotid gland as a source. The cystatins are a family of proteinase inhibitors

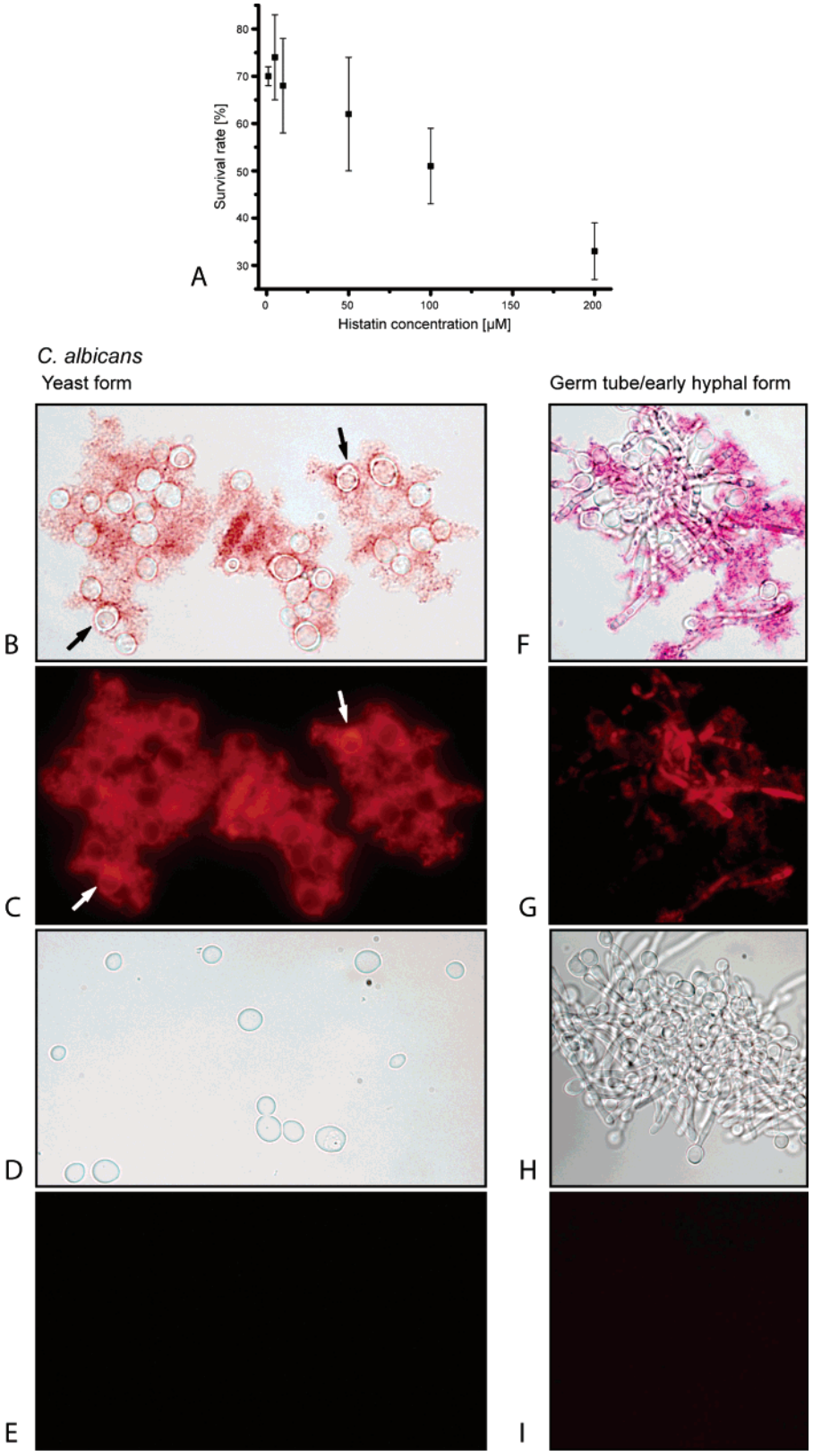

FIGURE 7: The novel histatin peptide octamer (HHGYKRKF) has dose-dependent candidacidal activity. (A) An aliquot of a *C. albicans* cell (yeast form) suspension was incubated with this peptide at 0−200 μM. After plating, the survival rate was determined by counting the number of colony-forming units. Cytotoxicity of the histatin peptide was also assessed by phloxine B dye exclusion. Yeast (left column) and germ tube/early hyphal forms (right column) of *C. albicans* were incubated with 200 μM peptide, and then either bright field (B, F) or fluorescence (C, G) microscopic images were obtained. The peptide rapidly killed *C. albicans* cells in both forms, as illustrated by intense staining with the vital dye, which quickly penetrated damaged cell membranes. Examples of intact dying or dead cells are indicated by the arrows. In the absence of the peptide, yeast and germ tube/early hyphal forms of *Candida* excluded the dye, as shown by the bright field (D, H) and fluorescence images (E, I).

that have been classified according to the compartment in which they are found: type 1, (mainly) intracellular; type 2, extracellular; and type 3, intravascular (*80*). Until recently, only type 2 cystatins (SA, SN, SA III, D) had been detected in saliva (*15*, *16*), and cystatin D was thought to be produced exclusively by the parotid gland (*81*). In 2004, Vitorino et al. (*17*) identified in whole saliva two type 1 cystatins (A, B) that were previously thought to remain in the intracellular compartment.

Additionally, our study revealed a wealth of peptides that, surprisingly, were derived from proteins other than the most abundant parotid components (e.g., α-amylase). Since parotid, in contrast to whole saliva, is amicrobial (*82*), these peptides are most likely formed before secretion and/or within the parotid duct. Based on sequence homology, the majority of peptides came from larger precursors, with processing at either the mRNA or the protein level a possibility. At least a portion of the peptides are produced by the latter mechanism: synthetic peptides with the same sequences as histatin precursors are cleaved into analogous fragments when they are incubated with parotid saliva in vitro (*44*).

Recently, Castagnola et al. (*43*) detected 24 histatin 3 fragments in whole saliva, of which six sequences are novel. The authors hypothesized that the lack of larger C-terminal fragments is evidence of a sequential cleavage pathway that specifically processes histatin 3. In contrast, our data revealed fragments representing putative cleavages throughout the entire histatin 3 sequence (Table 4, Figure 6). Finally, our results show that parotid proteins other than histatin 3 are processed into peptides (histatin 1 and several PRPs), suggesting that this phenomenon is more widespread than previously thought.

Together, these data suggest that the peptide repertoire could be used to monitor proteinase or proteinase inhibitor activities as well as polymorphisms at potential proteolytic cleavage sites, differential RNA splicing (*83*) or allelic gene-length variation (*84*). It is likely that a subset of oral diseases either impact or are associated with the processes that generate fragments of parotid proteins, making these peptides candidate biomarkers. In this context, the analysis of the low-molecular-weight fraction of human saliva is an important component of any experimental strategy for establishing the proteome of this body fluid. This concept is in line with the realization that "peptidomics" of plasma and cerebrospinal fluid reveals a wealth of hormones, cytokines, growth factors, and peptides with important biological functions (*85*).

Our data illustrate some of the many challenges presented by proteome cataloging projects. For example, in some cases we were unable to detect proteins that are known to be important components of parotid saliva. This category included a subset of the PRPs that are encoded by six genes clustered in a single region—the human salivary protein complex (*86*). Allelic variation, differential RNA processing, proteolytic processing, phosphorylation, and glycosylation produce an array of more than 30 different PRPs (*83*, *87*). With regard to protein fragments, only two of 18 PRPs previously identified (*46*) were found in our study. Differences in sample preparation (pooled vs individual specimens, differential ethanol precipitation vs ultrafiltration) and analysis (Edman degradation vs MS) may explain this discrepancy. Nevertheless, only peptide P-C (IB-8b), which is derived from the kallikrein-mediated processing of acidic PRP-1 (PRP-C) and the peptide GRPQGPPQQGGHQQ ($[MH]^+$ *m*/*z* 1471.7), also derived from PRP-1, were found in both studies. Clearly, the sheer size and complexity of protein ensembles means, in practical terms, that there is no single analytical separation scenario that will provide the perfect outcome of detecting all proteins and peptides present in a given system (*88*). Therefore, a combination of different, preferably orthogonal, approaches is needed to maximize the number of detected/identified species.

Finally, we note the clinical utility of compiling the human salivary proteome. For example, detailed knowledge of salivary composition will aid in the construction of artificial salivas for use by patients with xerostomia and salivary hypofunction, conditions that are commonly associated with head and neck radiotherapy (*89*), Sjögren's syndrome (*90*), and the use of antidepressants (*91*). In this regard, the efficacy and safety of including antimicrobial proteins in artificial salivas is under evaluation (*92*). Additionally, cataloging the salivary proteins and peptides from healthy individuals is the requisite first step that will allow subsequent studies designed to link changes in the proteome and peptidome to specific disease states (*4*, *93*). Evidence already exists that indicates this approach will be fruitful. Chen et al. (*94*) used MALDI TOF MS to compare saliva samples from patients with oral cancer with those from healthy control subjects. Studying the expression of specific salivary components, for example, the defensins, has demonstrated that this family of proteins has antibiotic, antifungal, and antiviral properties (*95*−*100*). Specifically, human neutrophil peptide-1 (HNP1) is elevated in the saliva of patients with squamous cell carcinoma and oral inflammatory conditions (*96*−*98*). Analysis of saliva from patients with neutropenia and periodontitis secondary to Morbus Kostmann shows that the samples lack the bactericidal peptide LL-37 and have reduced levels of HNP1-3 (*101*). Differences in proteolytic processing of basic PRPs from the human parotid gland have been associated with caries (*46*). Interestingly, changes in salivary composition have also been linked to other aspects of human health beyond the field of dentistry, including diagnosis of myocardial infarctions and angina (*102*) and the objective quantitation of pain levels (*5*). As such, saliva is an easily obtained biological fluid with the potential to contain a great deal of important information, coded in terms of proteins and peptides, about an individual's health.

ACKNOWLEDGMENT

We thank Dr. Katalin Medzihradszky for help with the interpretation of MS/MS data, Dr. Arnie Falick for technical assistance, and Dr. Katherine E. Williams and Applied Biosystems for access to MALDI TOF/TOF MS/MS instrumentation.

SUPPORTING INFORMATION AVAILABLE

Supplemental Table 1 presenting heterogeneity of α-amylase population in human parotid saliva. This material is available free of charge via the Internet at http://pubs.acs.org.

REFERENCES

1. Amerongen, A. V., and Veerman, E. C. (2002) Saliva-the defender of the oral cavity, *Oral Dis. 8*, 12−22.
2. Kaufman, E., and Lamster, I. B. (2000) Analysis of saliva for periodontal diagnosis—a review, *J. Clin. Periodontol. 27*, 453−465.

3. Kaufman, E., and Lamster, I. B. (2002) The diagnostic applications of saliva—a review, *Crit. Rev. Oral Biol. Med. 13*, 197−212.
4. Mandel, I. D. (1993) Salivary diagnosis: more than a lick and a promise, *J. Am. Dent. Assoc. 124*, 85−87.
5. Fischer, H. P., Eich, W., and Russell, I. J. (1998) A possible role for saliva as a diagnostic fluid in patients with chronic pain, *Semin. Arthritis Rheum. 27*, 348−359.
6. Nagler, R. M., Hershkovich, O., Lischinsky, S., Diamond, E., and Reznick, A. Z. (2002) Saliva analysis in the clinical setting: revisiting an underused diagnostic tool, *J. Invest. Med. 50*, 214−225.
7. Streckfus, C. F., and Bigler, L. R. (2002) Saliva as a diagnostic fluid, *Oral Dis. 8*, 69−76.
8. Rohlff, C. (2000) Proteomics in molecular medicine: applications in central nervous systems disorders, *Electrophoresis 21*, 1227−1234.
9. Yuan, X., Russell, T., Wood, G., and Desiderio, D. M. (2002) Analysis of the human lumbar cerebrospinal fluid proteome, *Electrophoresis 23*, 1185−1196.
10. Davis, M. T., Spahr, C. S., McGinley, M. D., Robinson, J. H., Bures, E. J., Beierle, J., Mort, J., Yu, W., Luethy, R., and Patterson, S. D. (2001) Towards defining the urinary proteome using liquid chromatography-tandem mass spectrometry. II. Limitations of complex mixture analyses, *Proteomics 1*, 108−117.
11. Spahr, C. S., Davis, M. T., McGinley, M. D., Robinson, J. H., Bures, E. J., Beierle, J., Mort, J., Courchesne, P. L., Chen, K., Wahl, R. C., Yu, W., Luethy, R., and Patterson, S. D. (2001) Towards defining the urinary proteome using liquid chromatography-tandem mass spectrometry. I. Profiling an unfractionated tryptic digest, *Proteomics 1*, 93−107.
12. Sinz, A., Bantscheff, M., Mikkat, S., Ringel, B., Drynda, S., Kekow, J., Thiesen, H. J., and Glocker, M. O. (2002) Mass spectrometric proteome analyses of synovial fluids and plasmas from patients suffering from rheumatoid arthritis and comparison to reactive arthritis or osteoarthritis, *Electrophoresis 23*, 3445−3456.
13. Vuadens, F., Benay, C., Crettaz, D., Gallot, D., Sapin, V., Schneider, P., Bienvenut, W. V., Lemery, D., Quadroni, M., Dastugue, B., and Tissot, J. D. (2003) Identification of biologic markers of the premature rupture of fetal membranes: proteomic approach, *Proteomics 3*, 1521−1525.
14. Liotta, L. A., Ferrari, M., and Petricoin, E. (2003) Clinical proteomics: written in blood, *Nature 425*, 905.
15. Yao, Y., Berg, E. A., Costello, C. E., Troxler, R. F., and Oppenheim, F. G. (2003) Identification of protein components in human acquired enamel pellicle and whole saliva using novel proteomics approaches, *J. Biol. Chem. 278*, 5300−5308.
16. Ghafouri, B., Tagesson, C., and Lindahl, M. (2003) Mapping of proteins in human saliva using two-dimensional gel electrophoresis and peptide mass fingerprinting, *Proteomics 3*, 1003−1015.
17. Vitorino, R., Lobo, M. J., Ferrer-Correira, A. J., Dubin, J. R., Tomer, K. B., Domingues, P. M., and Amado, F. M. (2004) Identification of human whole saliva protein components using proteomics, *Proteomics 4*, 1109−1115.
18. Kojima, T., Andersen, E., Sanchez, J. C., Wilkins, M. R., Hochstrasser, D. F., Pralong, W. F., and Cimasoni, G. (2000) Human gingival crevicular fluid contains MRP8 (S100A8) and MRP14 (S100A9), two calcium-binding proteins of the S100 family, *J. Dent. Res. 79*, 740−747.
19. Beeley, J. A., Khoo, K. S., and Lamey, P. J. (1991) 2-Dimensional electrophoresis of human parotid salivary proteins from normal and connective-tissue disorder subjects using immobilized pH gradients, *Electrophoresis 12*, 493−499.
20. Mogi, M., Hiraoka, B. Y., Fukasawa, K., Harada, M., Kage, T., and Chino, T. (1986) Two-dimensional electrophoresis in the analysis of a mixture of human sublingual and submandibular salivary proteins, *Arch. Oral Biol. 31*, 119−125.
21. International Human Genome Sequencing Consortium. (2004) Finishing the euchromatic sequence of the human genome, *Nature 431*, 931−945.
22. Venter, J. C., et al. (2001) The sequence of the human genome, *Science 291*, 1304−1351.
23. Lander, E. S., et al. (2001) Initial sequencing and analysis of the human genome, *Nature 409*, 860−921.
24. Adams, M. D., et al. (2000) The genome sequence of Drosophila melanogaster, *Science 287*, 2185−2195.
25. Bertozzi, C. R., and Kiessling, L. L. (2001) Chemical Glycobiology, *Science 291*, 2357.
26. Spiro, R. G. (2002) Protein glycosylation: nature, distribution, enzymatic formation, and disease implications of glycopeptide bonds, *Glycobiology 12*, 43R−56R.
27. Prakobphol, A., Thomsson, K. A., Hansson, G. C., Rosen, S. D., Singer, M. S., Phillips, N. J., Medzihradszky, K. F., Burlingame, A. L., Leffler, H., and Fisher, S. J. (1998) Human low-molecular-weight salivary mucin expresses the sialyl lewisx determinant and has L-selectin ligand activity, *Biochemistry 37*, 4916−4927.
28. Isemura, S., Saitoh, E., Sanada, K., and Minakata, K. (1991) Identification of full-sized forms of salivary (S-type) cystatins (cystatin SN, cystatin SA, cystatin S, and two phosphorylated forms of cystatin S) in human whole saliva and determination of phosphorylation sites of cystatin S, *J. Biochem. (Tokyo) 110*, 648−654.
29. Lamkin, M. S., and Oppenheim, F. G. (1994) Phosphorylation of salivary proteins by protein kinases., *J. Dent. Res. 73*, 191.
30. Drzymala, L., Castle, A., Cheung, J. C., and Bennick, A. (2000) Cellular phosphorylation of an acidic proline-rich protein, PRP1, a secreted salivary phosphoprotein, *Biochemistry 39*, 2023−2031.
31. Bennick, A., McLaughlin, A. C., Grey, A. A., and Madapallimattam, G. (1981) The location and nature of calcium-binding sites in salivary acidic proline-rich phosphoproteins, *J. Biol. Chem. 256*, 4741−4746.
32. Zahradnik, R. T., Moreno, E. C., and Burke, E. J. (1976) Effect of salivary pellicle on enamel subsurface demineralization in vitro, *J. Dent. Res. 55*, 664−670.
33. Shomers, J. P., Tabak, L. A., Levine, M. J., Mandel, I. D., and Hay, D. I. (1982) Properties of cysteine-containing phosphoproteins from human submandibular-sublingual saliva, *J. Dent. Res. 61*, 397−399.
34. Driscoll, J., Zuo, Y., Xu, T., Choi, J. R., Troxler, R. F., and Oppenheim, F. G. (1995) Functional comparison of native and recombinant human salivary histatin 1, *J. Dent. Res. 74*, 1837−1844.
35. Hay, D. I., Moreno, E. C., and Schlesinger, D. H. (1979) Phosphoprotein-inhibitors of calcium phosphate precipitation from salivary secretions., *Inorg. Perspect. Biol. Med. 2*, 271−285.
36. Schlesinger, D. H., Buku, A., Wyssbrod, H. R., and Hay, D. I. (1987) Chemical synthesis of phosphoseryl-phosphoserine, a partial analogue of human salivary statherin, a protein inhibitor of calcium phosphate precipitation in human saliva, *Int. J. Pept. Protein Res. 30*, 257−262.
37. Sabatini, L. M., and Azen, E. A. (1989) Histatins, a family of salivary histidine-rich proteins, are encoded by at least two loci (HIS1 and HIS2), *Biochem. Biophys. Res. Commun. 160*, 495−502.
38. Baum, B. J., Bird, J. L., Millar, D. B., and Longton, R. W. (1976) Studies on histidine-rich polypeptides from human parotid saliva, *Arch. Biochem. Biophys. 177*, 427−436.
39. Azen, E. A. (1973) Properties of salivary basic proteins showing polymorphism, *Biochem. Genet. 9*, 69−86.
40. Troxler, R. F., Offner, G. D., Xu, T., Vanderspek, J. C., and Oppenheim, F. G. (1990) Structural relationship between human salivary histatins, *J. Dent. Res. 69*, 2−6.
41. Xu, L., Lal, K., and Pollock, J. J. (1992) Histatins 2 and 4 are autoproteolytic degradation products of human parotid saliva, *Oral Microbiol. Immunol. 7*, 127−128.
42. Perinpanayagam, H. E., Van Wuyckhuyse, B. C., Ji, Z. S., and Tabak, L. A. (1995) Characterization of low-molecular-weight peptides in human parotid saliva, *J. Dent. Res. 74*, 345−350.
43. Castagnola, M., Inzitari, R., Rossetti, D. V., Olmi, C., Cabras, T., Piras, V., Nicolussi, P., Sanna, M. T., Pellegrini, M., Giardina, B., and Messana, I. (2004) A cascade of 24 histatins (histatin 3 fragments) in human saliva. Suggestions for a pre-secretory sequential cleavage pathway, *J. Biol. Chem. 279*, 41436−41443.
44. Xu, L., Lal, K., Santarpia, R. P., 3rd, and Pollock, J. J. (1993) Salivary proteolysis of histidine-rich polypeptides and the antifungal activity of peptide degradation products, *Arch. Oral Biol. 38*, 277−283.
45. Jensen, J. L., Lamkin, M. S., Troxler, R. F., and Oppenheim, F. G. (1991) Multiple forms of statherin in human salivary secretions, *Arch. Oral Biol. 36*, 529−534.
46. Ayad, M., Van Wuyckhuyse, B. C., Minaguchi, K., Raubertas, R. F., Bedi, G. S., Billings, R. J., Bowen, W. H., and Tabak, L. A. (2000) The association of basic proline-rich peptides from human parotid gland secretions with caries experience, *J. Dent. Res. 79*, 976−982.
47. Messana, I., Cabras, T., Inzitari, R., Lupi, A., Zuppi, C., Olmi, C., Fadda, M. B., Cordaro, M., Giardina, B., and Castagnola, M.

(2004) Characterization of the human salivary basic proline-rich protein complex by a proteomic approach, *J. Proteome Res. 3*, 792−800.
48. Lupi, A., Messana, I., Denotti, G., Schinina, M. E., Gambarini, G., Fadda, M. B., Vitali, A., Cabras, T., Piras, V., Patamia, M., Cordaro, M., Giardina, B., and Castagnola, M. (2003) Identification of the human salivary cystatin complex by the coupling of high-performance liquid chromatography and ion-trap mass spectrometry, *Proteomics 3*, 461−467.
49. Distler, W., and Kroncke, A. (1987) Biologically-active, low-molecular-weight peptides in human saliva, *J. Dent. Res. 66*, 603−604.
50. Nelson, R. W., and Vestal, M. L. (1991) Direct analysis of salivary proteins using matrix-assisted laser desorption time of flight mass spectrometry, presented at the 39th ASMS Conference on Mass Spectrometry and Allied Topics, May 19−24, Nashville, TN.
51. Gillece-Castro, B. L., Prakobphol, A., Burlingame, A. L., Leffler, H., and Fisher, S. J. (1991) Structure and bacterial receptor activity of a human salivary proline-rich glycoprotein, *J. Biol. Chem. 266*, 17358−17368.
52. Gorg, A., Postel, W., Weser, J., Gunther, S., Strahler, J. R., Hanash, S. M., and Somerlot, L. (1987) Elimination of point streaking on silver stained two-dimensional gels by addition of iodoacetamide to the equilibration buffer, *Electrophoresis 8*, 122−124.
53. Meyer, T. S., and Lamberts, B. L. (1965) Use of Coomassie brilliant blue R250 for the electrophoresis of microgram quantities of parotid saliva proteins on acrylamide-gel strips, *Biochim. Biophys. Acta 107*, 144−145.
54. Marshall, T., and Williams, K. M. (1987) Sodium dodecyl sulfate-polyacrylamide gel-electrophoresis of human salivary proteins including pink-violet components—range, distribution and response to 2-mercaptoethanol, *Electrophoresis 8*, 580−584.
55. Shatzman, A. R., and Henkin, R. I. (1983) The Proline-Rich, Glycine-Rich, and Glutamic Acid-Rich Pink- Violet Staining Proteins in Human-Parotid Saliva Are Phosphoproteins, *Biochem. Med. 29*, 182−193.
56. Henzel, W. J., Billeci, T. M., Stults, J. T., Wong, S. C., Grimley, C., and Watanabe, C. (1993) Identifying proteins from two-dimensional gels by molecular mass searching of peptide fragments in protein sequence databases, *Proc. Natl. Acad. Sci. U.S.A. 90*, 5011−5015.
57. James, P., Quadroni, M., Carafoli, E., and Gonnet, G. (1993) Protein identification by mass profile fingerprinting, *Biochem. Biophys. Res. Commun. 195*, 58−64.
58. Mann, M., Hojrup, P., and Roepstorff, P. (1993) Use of mass spectrometric molecular weight information to identify proteins in sequence databases, *Biol. Mass Spectrom. 22*, 338−345.
59. Pappin, D., Hojrup, P., and Bleasby, A. (1993) *Curr. Biol. 3*, 327.
60. Yates, J. R., 3rd, Speicher, S., Griffin, P. R., and Hunkapiller, T. (1993) Peptide mass maps: a highly informative approach to protein identification, *Anal. Biochem. 214*, 397−408.
61. Perkins, D. N., Pappin, D. J., Creasy, D. M., and Cottrell, J. S. (1999) Probability-based protein identification by searching sequence databases using mass spectrometry data, *Electrophoresis 20*, 3551−3567.
62. Clauser, K. R., Baker, P., and Burlingame, A. L. (1999) Role of accurate mass measurement (+/− 10 ppm) in protein identification strategies employing MS or MS/MS and database searching, *Anal. Chem. 71*, 2871−2882.
63. Kucsera, J., Yarita, K., and Takeo, K. (2000) Simple detection method for distinguishing dead and living yeast colonies, *J. Microbiol. Methods 41*, 19−21.
64. Bank, R. A., Hettema, E. H., Arwert, F., Amerongen, A. V., and Pronk, J. C. (1991) Electrophoretic characterization of posttranslational modifications of human parotid salivary alpha-amylase, *Electrophoresis 12*, 74−79.
65. Annan, R. S., and Carr, S. A. (1996) Phosphopeptide analysis by matrix-assisted laser desorption time-of-flight mass spectrometry, *Anal. Chem. 68*, 3413−3421.
66. Muller, D. R., Schindler, P., Coulot, M., Voshol, H., and van Oostrum, J. (1999) Mass spectrometric characterization of stathmin isoforms separated by 2D PAGE, *J. Mass Spectrom. 34*, 336−345.
67. Blom, N., Gammeltoft, S., and Brunak, S. (1999) Sequence and structure-based prediction of eukaryotic protein phosphorylation sites, *J. Mol. Biol. 294*, 1351−1362.
68. Oppenheim, F. G., Xu, T., McMillian, F. M., Levitz, S. M., Diamond, R. D., Offner, G. D., and Troxler, R. F. (1988) Histatins, a novel family of histidine-rich proteins in human parotid secretion. Isolation, characterization, primary structure, and fungistatic effects on Candida albicans, *J. Biol. Chem. 263*, 7472−7477.
69. Leymarie, N., Berg, E. A., McComb, M. E., O'Connor, P. B., Grogan, J., Oppenheim, F. G., and Costello, C. E. (2002) Tandem mass spectrometry for structural characterization of proline-rich proteins: application to salivary PRP-3, *Anal. Chem. 74*, 4124−4132.
70. Schenkels, L. C., Veerman, E. C., and Nieuw Amerongen, A. V. (1995) EP-GP and the lipocalin VEGh, two different human salivary 20-kDa proteins, *J. Dent. Res. 74*, 1543−1550.
71. Murphy, L. C., Tsuyuki, D., Myal, Y., and Shiu, R. P. (1987) Isolation and sequencing of a cDNA clone for a prolactin-inducible protein (PIP). Regulation of PIP gene expression in the human breast cancer cell line, T-47D, *J. Biol. Chem. 262*, 15236−15241.
72. Rathman, W. M., Van Zeyl, M. J., Van den Keybus, P. A., Bank, R. A., Veerman, E. C., and Nieuw Amerongen, A. V. (1989) Isolation and characterization of three non-mucinous human salivary proteins with affinity for hydroxyapatite, *J. Biol. Buccale 17*, 199−208.
73. Schenkels, L. C., Schaller, J., Walgreen-Weterings, E., Schadee-Eestermans, I. L., Veerman, E. C., and Nieuw Amerongen, A. V. (1994) Identity of human extra parotid glycoprotein (EP-GP) with secretory actin binding protein (SABP) and its biological properties, *Biol. Chem. Hoppe-Seyler 375*, 609−615.
74. Schenkels, L. C., Walgreen-Weterings, E., Oomen, L. C., Bolscher, J. G., Veerman, E. C., and Nieuw Amerongen, A. V. (1997) In vivo binding of the salivary glycoprotein EP-GP (identical to GCDFP-15) to oral and non-oral bacteria detection and identification of EP-GP binding species, *Biol. Chem. 378*, 83−88.
75. Autiero, M., Abrescia, P., and Guardiola, J. (1991) Interaction of seminal plasma proteins with cell surface antigens: presence of a CD4-binding glycoprotein in human seminal plasma, *Exp. Cell Res. 197*, 268−271.
76. Caputo, E., Manco, G., Mandrich, L., and Guardiola, J. (2000) A novel aspartyl proteinase from apocrine epithelia and breast tumors, *J. Biol. Chem. 275*, 7935−7941.
77. Hirai, K., Hussey, H. J., Barber, M. D., Price, S. A., and Tisdale, M. J. (1998) Biological evaluation of a lipid-mobilizing factor isolated from the urine of cancer patients, *Cancer Res. 58*, 2359−2365.
78. Hale, L. P., Price, D. T., Sanchez, L. M., Demark-Wahnefried, W., and Madden, J. F. (2001) Zinc alpha-2-glycoprotein is expressed by malignant prostatic epithelium and may serve as a potential serum marker for prostate cancer, *Clin. Cancer Res. 7*, 846−853.
79. Tada, T., Ohkubo, I., Niwa, M., Sasaki, M., Tateyama, H., and Eimoto, T. (1991) Immunohistochemical localization of Zn-alpha 2-glycoprotein in normal human tissues, *J. Histochem. Cytochem. 39*, 1221−1226.
80. Abrahamson, M., Alvarez-Fernandez, M., and Nathanson, C. M. (2003) Cystatins, *Biochem. Soc. Symp*. 179−199.
81. Freitas-Fernandes, L. B., Rundegren, J., Arnebrant, T., and Glantz, P. O. (1998) Delmopinol hydrochloride- and chlorhexidine digluconate-induced precipitation of salivary proteins of different molecular weights, *Acta Odontol. Scand. 56*, 2−8.
82. Kerr, A., and Wedderburn, D. (1958) Antibacterial factors in the secretions of human parotid and submaxillary glands, *Br. Dent. J. 4*, 321−326.
83. Maeda, N., Kim, H. S., Azen, E. A., and Smithies, O. (1985) Differential RNA splicing and post-translational cleavages in the human salivary proline-rich protein gene system, *J. Biol. Chem. 260*, 11123−11130.
84. Lyons, K. M., Stein, J. H., and Smithies, O. (1988) Length polymorphisms in human proline-rich protein genes generated by intragenic unequal crossing over, *Genetics 120*, 267−278.
85. Schulz-Knappe, P., Zucht, H. D., Heine, G., Jurgens, M., Hess, R., and Schrader, M. (2001) Peptidomics: the comprehensive analysis of peptides in complex biological mixtures, *Comb. Chem. High Throughput Screening 4*, 207−217.
86. Kim, H. S., Smithies, O., and Maeda, N. (1990) A physical map of the human salivary proline-rich protein gene cluster covers over 700 kbp of DNA, *Genomics 6*, 260−267.
87. Mamula, P. W., Morley, D. J., Larsen, S. H., and Karn, R. C. (1988) Expression of human salivary protein genes, *Biochem. Genet. 26*, 165−175.
88. Aebersold, R., and Mann, M. (2003) Mass spectrometry-based proteomics, *Nature 422*, 198−207.

89. Vissink, A., Jansma, J., Spijkervet, F. K., Burlage, F. R., and Coppes, R. P. (2003) Oral sequelae of head and neck radiotherapy, *Crit. Rev. Oral Biol. Med. 14*, 199−212.
90. Mahoney, E. J., and Spiegel, J. H. (2003) Sjogren's disease, *Otolaryngol. Clin. North Am. 36*, 733−745.
91. Peeters, F. P., deVries, M. W., and Vissink, A. (1998) Risks for oral health with the use of antidepressants, *Gen. Hosp. Psychiatry 20*, 150−154.
92. Tenovuo, J. (2002) Clinical applications of antimicrobial host proteins lactoperoxidase, lysozyme and lactoferrin in xerostomia: efficacy and safety, *Oral Dis. 8*, 23−29.
93. Mandel, I. D. (1993) Salivary diagnosis: promises, promises, *Ann. N.Y. Acad. Sci. 694*, 1−10.
94. Chen, Y. C., Li, T. Y., and Tsai, M. F. (2002) Analysis of the saliva from patients with oral cancer by matrix-assisted laser desorption/ionization time-of-flight mass spectrometry, *Rapid Commun. Mass Spectrom. 16*, 364−369.
95. Ganz, T. (2003) Defensins: antimicrobial peptides of innate immunity, *Nat. Rev. Immunol. 3*, 710−720.
96. Mizukawa, N., Sugiyama, K., Ueno, T., Mishima, K., Takagi, S., and Sugahara, T. (1999) Levels of human defensin-1, an antimicrobial peptide, in saliva of patients with oral inflammation, *Oral Surg., Oral Med., Oral Pathol., Oral Radiol. Endod. 87*, 539−543.
97. Mizukawa, N., Sugiyama, K., Fukunaga, J., Ueno, T., Mishima, K., Takagi, S., and Sugahara, T. (1998) Defensin-1, a peptide detected in the saliva of oral squamous cell carcinoma patients, *Anticancer Res. 18*, 4645−4649.
98. Mizukawa, N., Sugiyama, K., Ueno, T., Mishima, K., Takagi, S., and Sugahara, T. (1999) Defensin-1, an antimicrobial peptide present in the saliva of patients with oral diseases, *Oral Dis. 5*, 139−142.
99. Mathews, M., Jia, H. P., Guthmiller, J. M., Losh, G., Graham, S., Johnson, G. K., Tack, B. F., and McCray, P. B., Jr. (1999) Production of beta-defensin antimicrobial peptides by the oral mucosa and salivary glands, *Infect. Immun. 67*, 2740−2745.
100. Dale, B. A., and Krisanaprakornkit, S. (2001) Defensin antimicrobial peptides in the oral cavity, *J. Oral Pathol. Med. 30*, 321−327.
101. Putsep, K., Carlsson, G., Boman, H. G., and Andersson, M. (2002) Deficiency of antibacterial peptides in patients with morbus Kostmann: an observation study, *Lancet 360*, 1144−1149.
102. Jones, K. P., Reynolds, S. P., Gray, M., Hughes, K. T., Rolf, S., and Davies, B. H. (1994) Salivary PAF in acute myocardial infarction and angina: changes during hospital treatment and relationship to cardiac enzymes, *Thromb. Res. 75*, 503−511.
103. Edgerton, M., Koshlukova, S. E., Lo, T. E., Chrzan, B. G., Straubinger, R. M., and Raj, P. A. (1998) Candidacidal activity of salivary histatins. Identification of a histatin 5-binding protein on Candida albicans, *J. Biol. Chem. 273*, 20438−20447.
104. Murakami, Y., Takeshita, T., Shizukuishi, S., Tsunemitsu, A., and Aimoto, S. (1990) Inhibitory effects of synthetic histidine-rich peptides on hemagglutination by Bacteroides gingivalis 381, *Arch. Oral Biol. 35*, 775−777.
105. Raj, P. A., Edgerton, M., and Levine, M. J. (1990) Salivary histatin 5: dependence of sequence, chain length, and helical conformation for candidacidal activity, *J. Biol. Chem. 265*, 3898−3905.
106. Rothstein, D. M., Spacciapoli, P., Tran, L. T., Xu, T., Roberts, F. D., Dalla Serra, M., Buxton, D. K., Oppenheim, F. G., and Friden, P. (2001) Anticandida activity is retained in P-113, a 12-amino-acid fragment of histatin 5, *Antimicrob. Agents Chemother. 45*, 1367−1373.
107. Baum, B. J., Bird, J. L., and Longton, R. W. (1977) Evidence that the histidine-rich polypeptides of human parotid saliva are acinar secretory products of the parotid gland, *J. Dent Res. 56*, 877.

BI048176R